

Search for Excited Leptons in e^+e^- Annihilation at $\sqrt{s} = 161$ GeV

The L3 Collaboration

Abstract

A search for excited leptons e^* , μ^* , τ^* and ν_e^* in e^+e^- collisions at $\sqrt{s} = 161$ GeV is performed using the 10.8 pb^{-1} of data collected by the L3 detector at LEP. No evidence has been found for their existence. From an analysis of the expected $\ell^*\ell^*$ pair production in the channels $ee\gamma\gamma$, $\mu\mu\gamma\gamma$, $\tau\tau\gamma\gamma$, $eeWW$, and $\nu\nu\gamma\gamma$, the lower mass limits at 95% C.L. are 79.7 GeV for e^* , 79.9 GeV for μ^* , 79.3 GeV for τ^* and 71.3 GeV for ν_e^* assuming the same couplings as for standard leptons. From an analysis of the expected $\ell\ell^*$ single production in channels $ee\gamma$, $\mu\mu\gamma$, $\tau\tau\gamma$, $\nu_e eW$ and $\nu\nu\gamma$, the upper limits on the couplings λ/m_{ℓ^*} up to $m_{\ell^*} = 161$ GeV are determined.

(Submitted to Phys. Lett. B)

1 Introduction

The existence of excited leptons would be a clear signal for composite models, which can explain the number of families and make the fermion masses and weak mixing angles calculable [1]. The excited leptons e^* , μ^* , τ^* and ν^* have been extensively searched for at the LEP e^+e^- collider with $\sqrt{s} = 91$ GeV [2, 3] and $\sqrt{s} = 130 - 140$ GeV [4, 5] and at the HERA ep collider [6]. In this paper we report a search based on the 10.8 pb^{-1} of data collected by the L3 experiment at the centre of mass energy of 161 GeV.

An excited lepton ℓ^* is assumed to have spin $\frac{1}{2}$. It could have both a left and a right-handed component [7] or only a left-handed component as in the Standard Model. Since in the latter case the production cross section of excited lepton pairs is smaller, we use this assumption to make conservative estimates. An excited lepton, ℓ^* , is expected to decay immediately into its ground state, ℓ , by radiating a photon or a massive vector boson, Z or W.

At e^+e^- colliders, excited leptons can be produced either in pairs ($e^+e^- \rightarrow \ell^*\ell^*$) or singly ($e^+e^- \rightarrow \ell\ell^*$). For $\ell^*\ell^*$ pair production, the Z and γ are assumed to have the same coupling to an excited lepton pair $\ell^*\ell^*$ as to the standard lepton pair $\ell\ell$. The t -channel contribution for e^* and ν^* is neglected since the couplings $V\ell^*\ell$ are expected to be much smaller than normal couplings $V\ell\ell$ and $V\ell^*\ell^*$, where $V = \gamma, Z, W$. The lowest order pair production cross section can be found in ref. [1].

For single ℓ^* production, the effective Lagrangian [7] can be written as:

$$\mathcal{L}_{eff} = \sum_{V=\gamma,Z,W} \frac{e}{\Lambda} \bar{\Psi}_{\ell^*} \sigma^{\mu\nu} (C_{V\ell^*\ell} - D_{V\ell^*\ell} \gamma_5) \Psi_{\ell} \partial_{\mu} V_{\nu} + h.c.$$

where Λ is the composite mass scale and $C_{V\ell^*\ell}$ and $D_{V\ell^*\ell}$ are unknown coupling constants. The precise muon $g-2$ measurements impose $|C_{V\ell^*\ell}| = |D_{V\ell^*\ell}|$ [7, 8]. The absence of the electric dipole moment of electrons suggests that both $C_{V\ell^*\ell}$ and $D_{V\ell^*\ell}$ are real. We assume that the excited lepton and its corresponding excited neutrino are a weak doublet, therefore the coupling constants satisfy $C_{V\ell^*\ell} = D_{V\ell^*\ell}$, and we have:

$$C_{\gamma\ell^*\ell} = \frac{1}{2}(t_3 f + \frac{Y}{2} f'), \quad C_{Z\ell^*\ell} = \frac{1}{2}(t_3 f \cot\theta_W - \frac{Y}{2} f' \tan\theta_W), \quad C_{W\ell^*\ell} = \frac{f}{2\sqrt{2}\sin\theta_W},$$

where f and f' are the free parameters for SU(2) and U(1) respectively, t_3 is the third component of weak isospin of ℓ^* , Y is the hypercharge of ℓ^* , and θ_W is the weak mixing angle. Throughout this paper we assume that t_3 and Y are the same for ℓ and ℓ^* .

For excited charged leptons, we assume $f = f'$ in the above formula, so that $f/\Lambda (= \sqrt{2}\lambda/m_{\ell^*})$ is the only free parameter in the Lagrangian [9]. An excited charged lepton is expected to decay immediately into its corresponding standard lepton and a photon with a 100% branching ratio if its mass is smaller than that of the W. For higher mass, the decays $\ell^* \rightarrow Z\ell$ and $\ell^* \rightarrow W\nu$ become important and the branching ratio of $\ell^* \rightarrow \ell\gamma$ is then a function of m_{ℓ^*} [10]. For the excited neutrino ν^* , both $f = f'$ and $f \neq f'$ cases, described in detail in [4], are studied. In the former case the $\gamma\nu\nu^*$ coupling vanishes and $\nu^* \rightarrow \nu Z$ and $\nu^* \rightarrow eW$ are the only decay modes allowed, whereas in the latter case the $\gamma\nu\nu^*$ coupling exists and $\nu^* \rightarrow \nu\gamma$ decay would have a large branching ratio. In this analysis the searches are limited to the ν_e^* , which is assumed to be the lightest excited neutrino.

All the above processes have been generated by a Monte Carlo program according to the differential cross section of ref. [7] with an angular distribution of $1 + \cos\theta$ assigned to the ℓ^*

decay. The relevant branching ratios of ℓ^* decays are taken from ref. [10]. The subsequent τ decays are simulated by the TAUOLA and KORALZ Monte Carlo programs [11] and the hadronic fragmentation and decays are simulated by the JETSET Monte Carlo program [12]. The effect of initial state radiation is not included in the Monte Carlo generators but is taken into account in our cross section calculations. The generated events have been passed through the L3 detector simulation [13] which includes the effects of energy loss, multiple scattering, interactions and decays in the detector and the beam pipe.

2 The L3 Detector

The L3 detector is described in detail in ref. [14]. It consists of a silicon microstrip vertex detector, a central tracking chamber (TEC), a high resolution electromagnetic calorimeter composed of bismuth germanium oxide (BGO) crystals, plastic scintillation counters, a uranium hadron calorimeter with proportional wire chamber readout and a precise muon spectrometer. These detectors are installed in a 12 m diameter solenoid magnet which provides a uniform field of 0.5 T along the beam direction.

The BGO electromagnetic calorimeter covers the polar angle from 11° to 169° . It is divided into a barrel ($42^\circ < \theta < 138^\circ$) and endcaps ($11^\circ < \theta < 38^\circ$, $142^\circ < \theta < 169^\circ$). The energy resolution for photons and electrons is less than 2% for energies above 1 GeV. The angular resolution of electromagnetic clusters is better than 0.5° for energies above 1 GeV. The hadron calorimeter covers the polar angle from 5.5° to 174.5° . It measures the event energy, with the help of TEC and BGO, with a resolution of about 10% at 91 GeV. The muon chambers cover the polar angle from 22° to 158° . They are divided into barrel ($36^\circ < \theta < 144^\circ$), forward ($22^\circ < \theta < 36^\circ$) and backward ($144^\circ < \theta < 158^\circ$) regions.

3 Pair Production of Excited Leptons

In the L3 detector an electron is identified as an electromagnetic shower with a matched track within 5° in the $r\phi$ projection. If the shower is isolated from all tracks by more than 15° in the $r\phi$ projection, it is identified as a photon. Muons are identified from tracks in the muon chambers with measurements in both the $r\phi$ and rz projections. The transverse and the longitudinal distances of closest approach to the interaction vertex are both required to be less than 200 mm. For tau identification, a jet clustering algorithm [15] is used which groups neighbouring calorimeter energy depositions. The algorithm normally reconstructs one jet for a single isolated electron, photon, muon, high energy tau or hadronic jet.

Event selection for the reaction $e^+e^- \rightarrow \ell^*\ell^* \rightarrow \ell\ell\gamma\gamma$ is based on the fact that these processes contain two leptons and two photons. The Standard Model background from lepton pair production with initial and final state radiation can be efficiently reduced by requiring two energetic photons.

To remove the background from two-photon collisions, in all channels except in the single photon final state, the visible energy of the event is required to be more than half of the beam energy.

3.1 Pair Production of e^*

Event selection for the reaction $e^+e^- \rightarrow e^*e^* \rightarrow ee\gamma\gamma$ requires the following criteria:

- (i) there must be two electrons and two photons, each with an energy greater than $0.2E_{\text{beam}}$, where E_{beam} is the beam energy;
- (ii) for at least one of the two possible e, γ permutations for $m_1(e_1, \gamma_1), m_2(e_2, \gamma_2)$, the mass difference $m_1 - m_2$ must be less than 10 GeV and the average mass must be greater than 50 GeV.

No events pass the selection. The main background is due to radiative Bhabha events $e^+e^- \rightarrow ee\gamma\gamma$. Owing to uncertainties of Monte Carlo predictions for hard radiative Bhabha processes, we conservatively make no background subtraction in calculating the upper limit.

The detection efficiency for the signal is estimated from Monte Carlo to be 51%, which is slightly dependent on the mass of the e^* . The decay branching ratio for $e^* \rightarrow e\gamma$ is close to 100% for the mass region concerned.

Taking into account the luminosity, the efficiency and the production cross section of e^* , we obtain the number of expected e^* as a function of m_{e^*} . From Poisson statistics, we determine the lower mass limit for excited electrons at 95% Confidence Level (C.L.) to be 79.7 GeV.

3.2 Pair Production of μ^*

Event selection for the reaction $e^+e^- \rightarrow \mu^*\mu^* \rightarrow \mu\mu\gamma\gamma$ requires the following criteria:

- (i) there are exactly two tracks in the central tracking chamber, with at least one being an identified muon with an energy greater than 20 GeV;
- (ii) there are at least two photons with energies greater than $0.2E_{\text{beam}}$;
- (iii) if the two muons are measured by the muon chambers, cut (ii) in section 3.1 is applied for muons; if only one muon is measured, at least one $\mu\gamma$ combination must have an invariant mass between 50 GeV and 100 GeV.

No events pass the selection. The main background is due to radiative dimuon events $e^+e^- \rightarrow \mu\mu\gamma\gamma$. A total of 0.1 events is predicted from the KORALZ Monte Carlo program.

The detection efficiency for μ^* is estimated from a Monte Carlo study to be 60%, independent of the mass of the μ^* . The decay branching ratio for $\mu^* \rightarrow \mu\gamma$ is close to 100% for the mass region concerned. We determine the lower mass limit for excited muons at 95% C.L. to be 79.9 GeV.

3.3 Pair Production of τ^*

Event selection for the reaction $e^+e^- \rightarrow \tau^*\tau^* \rightarrow \tau\tau\gamma\gamma$ requires the following criteria:

- (i) the number of tracks is at least 2 and at most 7; there is at least one tau with energy deposition in the calorimeters not consistent with that of a muon; at least one tau has an energy greater than $0.2E_{\text{beam}}$;
- (ii) in the electromagnetic calorimeter, there are at least two photons with energies greater than $0.2E_{\text{beam}}$; total visible energy must be less than 85% of the centre of mass energy;
- (iii) if two tau jets are identified, cut (ii) in section 3.1 is applied for tau leptons; if only one tau jet is identified, at least one $\tau\gamma$ combination must have an invariant mass between 50 GeV and 100 GeV.

No events pass the selection. The background from radiative $\tau\tau$ events, $e^+e^- \rightarrow \tau\tau\gamma\gamma$, is estimated to be 0.1 events using the KORALZ program.

The detection efficiency for τ^* is estimated to be 40%, independent of the mass of τ^* . The decay branching ratio of $\tau^* \rightarrow \tau\gamma$ is close to 100% for the mass region concerned. We determine the lower mass limit for excited taus at 95% C.L. to be 79.4 GeV.

3.4 Pair Production of ν_e^*

For the event selection of excited electron neutrinos in the eW decay mode, the jet cluster algorithm used in the tau analysis is used. An isolated electron is defined as being more than 15° away from any other calorimetric cluster. The branching ratio for the eW decay mode ($f = f'$) rises from 72% at $m_{\nu_e^*} = 60$ GeV to 80% at $m_{\nu_e^*} = 80$ GeV. For the $\nu\gamma$ decay mode ($f \neq f'$), the branching ratio is close to 100% for the mass region concerned.

Event selection for the reaction $e^+e^- \rightarrow \nu_e^*\nu_e^* \rightarrow eeWW$ requires the following criteria:

- (i) the number of tracks must be at least 4 and the number of jets must be at least 3; the polar angle of the missing momentum must satisfy $|\cos\theta| < 0.95$;
- (ii) there must be at least one isolated electron with an energy between 5 GeV and 50 GeV to remove $q\bar{q}(\gamma)$ background with a converted photon; the number of jets must be at least 5 if there is no identified second electron with an energy greater than 1 GeV.

No events pass the selection. The background from the two-photon process is predicted to be negligible, 0.4 events are predicted from hadronic events and 0.3 events are predicted from W pair production [16] as estimated from Monte Carlo studies.

The detection efficiency is estimated from Monte Carlo to be 46%. The efficiency decreases to 18% at $m_{\nu_e^*} = 80$ GeV where the production and decay of a W at its energy threshold reduces the production of isolated electrons of sufficient energy. The decay branching ratio for $\nu_e^* \rightarrow eW$ is about 74% in the mass region concerned. The lower mass limit for excited neutrinos at 95% C.L., combined with our previous data [4], is determined to be 64.6 GeV.

Event selection for the reaction $e^+e^- \rightarrow \nu_e^*\nu_e^* \rightarrow \nu_e\nu_e\gamma\gamma$ requires the following criteria:

- (i) there are two photons in the barrel region each with an energy greater than 20 GeV; there are no tracks in the central tracking chamber;
- (ii) the energy deposited in the electromagnetic calorimeter must be less than 75% of the centre of mass energy and the energy deposited in the hadron calorimeter caused by the leakage of the electromagnetic showers must be less than 15 GeV.

No events pass the selection. The main background is due to the radiative $\nu\nu$ events, $e^+e^- \rightarrow \nu\nu\gamma\gamma$. A total of 0.2 events are predicted from KORALZ.

The detection efficiency is estimated to be 50%. It is slightly dependent on the mass of the ν_e^* . The decay branching ratio of $\nu_e^* \rightarrow \nu_e\gamma$ is 100% in the mass region concerned. We determine the lower mass limit for excited neutrinos to be 71.3 GeV at 95% C.L.

4 Single Production of Excited Leptons

Event selection for the reaction of $e^+e^- \rightarrow \ell\ell^* \rightarrow \ell\ell\gamma$ is based on the fact that these processes contain one energetic photon plus leptons. The photon is required to be in the barrel region and to have an energy more than 25 GeV and no other photons present.

4.1 Single Production of e^*

Event selection for the reaction $e^+e^- \rightarrow ee^* \rightarrow ee\gamma$ requires the following criteria:

- (i) there is at least one electron with an energy greater than 25 GeV and the number of tracks is at most 2;
- (ii) the total energy deposited in the hadron calorimeter caused by leakage of the electromagnetic shower must be less than 10 GeV;
- (iii) for events with only one observed electron, the thrust axis of the event must be within the barrel region.

A total of 29 events pass the selection; 23 of them have only one visible electron. A Monte Carlo calculation utilizing the TEE program [17] predicts 15.6 background events passing the selection cuts. Fig. 1a shows the invariant mass, $m_{e\gamma}$, of all combinations together with only the TEE prediction for the background. No significant structure is observed. The mass resolution for e^* is about 1 GeV, estimated from Monte Carlo events. We use the mass resolution and conservatively make only the background subtraction from the TEE prediction in calculating the upper limit.

The detection efficiency is estimated from Monte Carlo to be 51% at $m_{e^*} = 90$ GeV and 67% at $m_{e^*} = 160$ GeV. The decay branching ratio of $e^* \rightarrow e\gamma$ changes from 88% at $m_{e^*} = 90$ GeV to 38% at $m_{e^*} = 160$ GeV. Combining our present data with that for $\sqrt{s} = M_Z$ and $\sqrt{s} = 130 - 140$ GeV [2, 4] and taking into account the luminosity, the efficiency and the branching ratio, the upper limit of the coupling constant λ/m_{e^*} at 95% C.L. as a function of m_{e^*} is shown in Fig. 2.

4.2 Single Production of μ^*

Event selection for the reaction $e^+e^- \rightarrow \mu\mu^* \rightarrow \mu\mu\gamma$ requires the following criteria:

- (i) there is at least one identified muon with momentum greater than 15 GeV, and the number of tracks is at most 2;
- (ii) the total energy deposited in the hadron calorimeter must be less than 25 GeV;
- (iii) the polar angle of the missing momentum must satisfy $|\cos\theta| < 0.95$.

A total of 4 events pass the selection. The main background is due to radiative dimuon events $e^+e^- \rightarrow \mu\mu\gamma$, which is predicted from KORALZ to be 5.9 events. Fig. 1b shows the invariant mass, $m_{\mu\gamma}$, of all combinations together with the Monte Carlo prediction for the background. The mass resolution for μ^* is about 3 GeV for muons in the barrel (90% of observed events). No significant structure can be seen from the plot. We conclude that the observed events are compatible with the expected background.

The detection efficiency for a singly produced μ^* is estimated to be 62%. The efficiency decreases to 57% at a μ^* mass close to the centre of mass energy. The decay branching ratio of $\mu^* \rightarrow \mu\gamma$ changes from 88% at $m_{\mu^*} = 90$ GeV to 38% at $m_{\mu^*} = 160$ GeV. Combined with our previous data [2,4], we obtain an upper limit at 95% C.L. for the coupling constant λ/m_{μ^*} as a function of m_{μ^*} , as shown in Fig. 2.

4.3 Single Production of τ^*

Event selection for the reaction $e^+e^- \rightarrow \tau\tau^* \rightarrow \tau\tau\gamma$ requires the following criteria:

- (i) at least one tau jet energy must be greater than 2 GeV;
- (ii) the number of tracks must be at least 2 and at most 7, the number of clusters in the electromagnetic calorimeter must be less than 15;
- (iii) the total energy deposited in the electromagnetic calorimeter must be less than 85% of the centre of mass energy; the thrust axis of the event must be in the barrel region.

A total of 8 events pass the selection. The main background is due to radiative $\tau\tau$ events, $e^+e^- \rightarrow \tau\tau\gamma$, and is estimated to be 10.4 events by KORALZ. After applying kinematic constraints, we estimate the mass resolution of τ^* to be about 2 GeV from Monte Carlo events. Fig. 1c shows the invariant mass of the 8 selected events for all $\tau\gamma$ combinations, together with the Monte Carlo prediction for background. No structure is seen in the plot. We conclude that all events are compatible with the expected background.

The detection efficiency for a singly produced τ^* is estimated to be 52%, independent of the mass of the τ^* . The decay branching ratio of $\tau^* \rightarrow \tau\gamma$ changes from 88% at $m_{\tau^*} = 90$ GeV to 38% at $m_{\tau^*} = 159$ GeV. Combined with our previous data [2,4], we obtain an upper limit at 95% C.L. for the coupling constant λ/m_{τ^*} as a function of m_{τ^*} , as shown in Fig. 2.

4.4 Single Production of ν_e^*

Event selection for the reaction $e^+e^- \rightarrow \nu_e\nu_e^* \rightarrow \nu_e eW$ requires the following criteria:

- (i) there must be exactly one isolated electron with an energy greater than 5 GeV. The polar angle of the missing momentum must satisfy $|\cos\theta| < 0.95$.
- (ii) if the W decays leptonically, i.e. the number of tracks is less than 5, there must be only two jets in the event and their acoplanarity angle must satisfy $\cos\phi < 0.9$;
- (iii) if the W decays hadronically, i.e. the number of tracks is greater than or equal to 5 and there must be three jets in the event, each with an energy greater than 5 GeV.

A total of 6 events pass the selection. Backgrounds are predicted to be 4.1 events from W pair production [16] and 1.5 events from hadronic events. The backgrounds from $\tau\tau$ and two-photon collisions are negligible.

The detection efficiency is estimated to be 33% at $m_{\nu_e^*} = 90$ GeV and 44% at $m_{\nu_e^*} > 110$ GeV. The decay branching ratio of $\nu_e^* \rightarrow eW$ is more than 95% at $m_{\nu_e^*} = 90$ GeV and decreases to 64% at $m_{\nu_e^*} = 160$ GeV. Combined with our previous data [2,4], we obtain an upper limit at 95% C.L. for the coupling constant $\lambda/m_{\nu_e^*}$ as a function of $m_{\nu_e^*}$, as shown in Fig. 2.

Event selection for the reaction $e^+e^- \rightarrow \nu_e\nu_e^* \rightarrow \nu_e\nu_e\gamma$ requires the following criteria:

- (i) there must be only one photon in the barrel region with an energy greater than $0.2E_{\text{beam}}$;
- (ii) the total energy deposited in the hadron calorimeter caused by leakage of electromagnetic showers must be less than 10 GeV.

A total of 32 events pass the selection. The background is mainly due to radiative neutrino events $e^+e^- \rightarrow \nu\nu\gamma$, and $e^+e^- \rightarrow \gamma\gamma$ with one γ missing in the beam pipe. For radiative neutrino events there are 25.9 predicted from NNGSTR [18] consistent with the 26.1 predicted from KORALZ [11]. The number of events predicted for $e^+e^- \rightarrow \gamma\gamma$ background is 1.4 using the GGG generator [19]. We conclude that all events are compatible with the expected background.

The detection efficiency is estimated to be 73%. It is slightly dependent on the mass of the ν_e^* and is the same for both $f = 0$ and $f' = 0$. For $f = 0$, the decay branching ratio of $\nu_e^* \rightarrow \nu_e\gamma$ is 100% at $m_{\nu_e^*} < 91$ GeV and decreases to 86% at $m_{\nu_e^*} = 160$ GeV. For $f' = 0$, the decay branching ratio is 100% at $m_{\nu_e^*} < 80$ GeV and decreases to 12% at $m_{\nu_e^*} = 160$ GeV. Since it is not possible to reconstruct the $\nu\gamma$ invariant mass, we derive the upper limit on the basis of 32 observed events with 25.9 expected background events. An upper limit is obtained for the coupling constant $\lambda/m_{\nu_e^*}$ at 95% C.L. as a function of $m_{\nu_e^*}$ for both $f = 0$ and $f' = 0$. The result is shown in Fig. 3, in which $\lambda = f$ if $f' = 0$, and $\lambda = f'$ if $f = 0$.

5 Conclusion

We see no evidence for excited electrons, muons, taus or electron neutrinos; the observed events are consistent with Standard Model expectations. From pair production searches the lower mass limits at 95% C.L. are found to be 79.7 GeV for e^* , 79.9 GeV for μ^* , 79.3 GeV for τ^* , 64.6 GeV (eW decay mode) and 71.3 GeV ($\nu_e\gamma$ decay mode) for ν_e^* . From single production searches, we derived upper limits on the couplings λ/m_{ℓ^*} in the range of $(10^{-4} - 1)$ GeV $^{-1}$ for ℓ^* masses up to 161 GeV. Our results are in agreement with similar searches performed at the same energy [20].

6 Acknowledgments

We wish to congratulate the CERN accelerator divisions for the successful upgrade of LEP at the energy of $\sqrt{s} = 161$ GeV and to express our gratitude for the excellent performance of the machine. We acknowledge with appreciation the effort of all engineers, technicians and support staff who have participated in the construction and maintenance of this experiment. Those of us who are not from member states thanks CERN for its hospitality and help.

The L3 Collaboration:

M. Acciarri,²⁸ O. Adriani,¹⁷ M. Aguilar-Benitez,²⁷ S. Ahlen,¹¹ B. Alpat,³⁵ J. Alcaraz,²⁷ G. Alemani,²³ J. Allaby,¹⁸ A. Aloisio,³⁰ G. Alverson,¹² M. G. Alvigi,³⁰ G. Ambrosi,²⁰ H. Anderhub,⁵⁰ V. P. Andreev,³⁹ T. Angelescu,¹³ F. Anselmo,⁹ D. Antreasyan,⁹ A. Arefiev,²⁹ T. Azemoon,³ T. Aziz,¹⁰ P. Bagnaia,³⁸ L. Baksay,⁴⁵ R. C. Ball,³ S. Banerjee,¹⁰ K. Banicz,⁴⁷ R. Barillere,¹⁸ L. Barone,³⁸ P. Bartalini,³⁵ A. Baschirotto,²⁸ M. Basile,⁹ R. Battiston,³⁵ A. Bay,²³ F. Becattini,¹⁷ U. Becker,¹⁶ F. Behner,⁵⁰ J. Berdugo,²⁷ P. Berges,¹⁶ B. Bertucci,¹⁸ B. L. Betev,⁵⁰ S. Bhattacharya,¹⁰ M. Biasini,¹⁸ A. Biland,⁵⁰ G. M. Bilei,³⁵ J. J. Blaising,¹⁸ S. C. Blyth,³⁶ G. J. Bobbink,² R. Bock,¹ A. Böhm,¹ B. Borgia,³⁸ A. Boucham,⁴ D. Bourilkov,⁵⁰ M. Bourquin,²⁰ D. Boutigny,⁴ S. Braccini,²⁰ J. G. Branson,⁴¹ V. Brigljevic,⁵⁰ I. C. Brock,³⁶ A. Buffini,¹⁷ A. Buijs,⁴⁶ J. D. Burger,¹⁶ W. J. Burger,²⁰ J. Busenitz,⁴⁵ X. D. Cai,¹⁶ M. Campanelli,⁵⁰ M. Capell,¹⁶ G. Cara Romeo,⁹ M. Caria,³⁵ G. Carlino,³⁰ A. M. Cartacci,¹⁷ J. Casaus,²⁷ G. Castellini,¹⁷ F. Cavallari,³⁸ N. Cavallo,³⁰ C. Cecchi,²⁰ M. Cerrada,²⁷ F. Cesaroni,²⁴ M. Chamizo,²⁷ A. Chan,⁵² Y. H. Chang,⁵² U. K. Chaturvedi,¹⁹ S. V. Chekanov,³² M. Chemarin,²⁶ A. Chen,⁵² G. Chen,⁷ G. M. Chen,⁷ H. F. Chen,²¹ H. S. Chen,⁷ M. Chen,¹⁶ G. Chiefari,³⁰ C. Y. Chien,⁵ M. T. Choi,⁴⁴ L. Cifarelli,⁴⁰ F. Cindolo,⁹ C. Civinini,¹⁷ I. Clare,¹⁶ R. Clare,¹⁶ H. O. Cohn,³³ G. Coignet,⁴ A. P. Colijn,² N. Colino,²⁷ V. Commichau,¹ S. Costantini,³² F. Cotorobai,¹³ B. de la Cruz,²⁷ A. Csilling,¹⁴ T. S. Dai,¹⁶ R. D'Alessandro,¹⁷ R. de Asmundis,³⁰ A. Degré,⁴ K. Deiters,⁴⁸ P. Denes,³⁷ F. DeNotaristefani,³⁸ D. DiBitonto,⁴⁵ M. Diemoz,³⁸ D. van Dierendonck,² F. Di Lodovico,⁵⁰ C. Dionisi,³⁸ M. Dittmar,⁵⁰ A. Dominguez,⁴¹ A. Doria,³⁰ I. Dorne,⁴ M. T. Dova,^{19,4} E. Drago,³⁰ D. Duchesneau,⁴ P. Duinker,² I. Duran,⁴² S. Dutta,¹⁰ S. Easo,³⁵ Yu. Efremenko,³³ H. El Mamouni,²⁶ A. Engler,³⁶ F. J. Eppling,¹⁶ F. C. Erné,² J. P. Ernenwein,²⁶ P. Extermann,²⁰ M. Fabre,⁴⁸ R. Faccini,³⁸ S. Falciano,³⁸ A. Favara,¹⁷ J. Fay,²⁶ O. Fedin,³⁹ M. Felcini,⁵⁰ B. Fenyi,⁴⁵ T. Ferguson,³⁶ D. Fernandez,²⁷ F. Ferroni,³⁸ H. Fesefeldt,¹ E. Fiandrini,³⁵ J. H. Field,²⁰ F. Filthaut,³⁶ P. H. Fisher,¹⁶ G. Forconi,¹⁶ L. Fredj,²⁰ K. Freudenreich,⁵⁰ C. Furetta,²⁸ Yu. Galaktionov,^{29,16} S. N. Ganguli,¹⁰ P. Garcia-Abia,²⁷ S. S. Gau,¹² S. Gentile,³⁸ J. Gerald,⁵ N. Gheordanescu,¹³ S. Giagu,³⁸ S. Goldfarb,²³ J. Goldstein,¹¹ Z. F. Gong,²¹ A. Gougas,⁵ G. Gratta,³⁴ M. W. Gruenewald,⁸ V. K. Gupta,³⁷ A. Gurtu,¹⁰ L. J. Gutay,⁴⁷ B. Hartmann,¹ A. Hasan,³¹ D. Hatzifotiadou,⁹ T. Hebbeker,⁸ A. Hervé,¹⁸ W. C. van Hoek,³² H. Hofer,⁵⁰ H. Hoorani,³⁶ S. R. Hou,⁵² G. Hu,⁵ V. Innocente,¹⁸ H. Janssen,⁴ K. Jenkes,¹ B. N. Jin,⁷ L. W. Jones,³ P. de Jong,¹⁸ I. Josa-Mutuberria,²⁷ A. Kasser,²³ R. A. Khan,¹⁹ D. Kamrad,⁴⁹ Yu. Kamyshev,³³ J. S. Kapustinsky,²⁵ Y. Karyotakis,⁴ M. Kaur,^{19,4} M. N. Kienzle-Focacci,²⁰ D. Kim,⁵ J. K. Kim,⁴⁴ S. C. Kim,⁴⁴ Y. G. Kim,⁴⁴ W. W. Kinnison,²⁵ A. Kirkby,³⁴ D. Kirkby,³⁴ J. Kirkby,¹⁸ D. Kiss,¹⁴ W. Kittel,³² A. Klimentov,^{16,29} A. C. König,³² I. Korolko,²⁹ V. Koutsenko,^{16,29} R. W. Kraemer,³⁶ W. Krenz,¹ A. Kunin,^{16,29} P. Ladron de Guevara,²⁷ G. Landi,¹⁷ C. Lapoint,¹⁶ K. Lassila-Perini,⁵⁰ P. Laurikainen,²² M. Lebeau,¹⁸ A. Lebedev,¹⁶ P. Lebrun,²⁶ P. Lecomte,⁵⁰ P. Lecoq,¹⁸ P. Le Coultre,⁵⁰ J. S. Lee,⁴⁴ K. Y. Lee,⁴⁴ C. Leggett,³ J. M. Le Goff,¹⁸ R. Leiste,⁴⁹ E. Leonardi,³⁸ P. Levchenko,³⁹ C. Li,²¹ E. Lieb,⁴⁹ W. T. Lin,⁵² F. L. Linde,^{2,18} L. Lista,³⁰ Z. A. Liu,⁷ W. Lohmann,⁴⁹ E. Longo,³⁸ W. Lu,³⁴ Y. S. Lu,⁷ K. Lübelmeyer,¹ C. Luci,³⁸ D. Luckey,¹⁶ L. Luminari,³⁸ W. Lustermaier,³⁸ W. G. Ma,²¹ M. Maity,¹⁰ G. Majumder,¹⁰ L. Malgeri,³⁸ A. Malinin,²⁹ C. Mañá,²⁷ D. Mangeol,³² S. Mangla,¹⁰ P. Marchesini,⁵⁰ A. Marin,¹¹ J. P. Martin,²⁶ F. Marzano,³⁸ G. G. G. Massaro,² D. McNally,¹⁸ S. Mele,³⁰ L. Merola,³⁰ M. Meschini,⁷ W. J. Metzger,³² M. von der Mey,¹ Y. Mi,²³ A. Mihul,¹³ A. J. W. van Mil,³² G. Mirabelli,³⁸ J. Mnich,¹⁸ P. Molnar,⁸ B. Monteleoni,¹⁷ R. Moore,³ S. Morganti,³⁸ T. Moulik,¹⁰ R. Mount,³⁴ S. Müller,¹ F. Muheim,²⁰ A. J. M. Muijs,² E. Nagy,¹⁴ S. Nahn,¹⁶ M. Napolitano,³⁰ F. Nessi-Tedaldi,⁵⁰ H. Newman,³⁴ T. Niessen,¹ A. Nippe,¹ A. Nisati,³⁸ H. Nowak,⁴⁹ H. Opitz,¹ G. Organtini,³⁸ R. Ostonen,²² D. Pandoulas,¹ S. Paoletti,³⁸ P. Paolucci,³⁰ H. K. Park,³⁶ G. Pascale,³⁸ G. Passaleva,¹⁷ S. Patricelli,³⁰ T. Paul,² M. Pauluzzi,³⁵ C. Paus,¹ F. Pauss,⁵⁰ D. Peach,¹⁸ Y. J. Pei,¹ S. Pensotti,²⁸ D. Perret-Gallix,⁴ B. Petersen,³² S. Petrak,⁸ A. Pevsner,⁵ D. Piccolo,³⁰ M. Pieri,¹⁷ J. C. Pinto,³⁶ P. A. Piroué,³⁷ E. Pistolesi,²⁸ V. Plyaskin,²⁹ M. Pohl,⁵⁰ V. Pojidaev,^{29,17} H. Postema,¹⁶ N. Produit,²⁰ D. Prokofiev,³⁹ G. Rahal-Callot,⁵⁰ P. G. Rancoita,²⁸ M. Rattaggi,²⁸ G. Raven,⁴¹ P. Razis,³¹ K. Read,³³ D. Ren,⁵⁰ M. Rescigno,³⁸ S. Reucroft,¹² T. van Rhee,⁴⁶ S. Riemann,⁴⁹ K. Riles,³ O. Rind,³ S. Ro,⁴⁴ A. Robohm,⁵⁰ J. Rodin,¹⁶ F. J. Rodriguez,²⁷ B. P. Roe,³ L. Romero,²⁷ S. Rosier-Lees,⁴ Ph. Rossetlet,²³ W. van Rossum,⁴⁶ S. Roth,¹ J. A. Rubio,¹⁸ H. Rykaczewski,⁵⁰ J. Salicio,¹⁸ E. Sanchez,²⁷ M. P. Sanders,³² A. Santocchia,³⁵ M. E. Sarakinos,²² S. Sarkar,¹⁰ M. Sassowsky,¹ G. Sauvage,⁴ C. Schäfer,¹ V. Schegelsky,³⁹ S. Schmidt-Kaerst,¹ D. Schmitz,¹ P. Schmitz,¹ M. Schneegans,⁴ N. Scholz,⁵⁰ H. Schopper,⁵¹ D. J. Schotanus,³² J. Schwenke,¹ G. Schwering,¹ C. Sciacca,³⁰ D. Sciarrino,²⁰ L. Servoli,³⁵ S. Shevchenko,³⁴ N. Shivarov,⁴³ V. Shoutko,²⁹ J. Shukla,²⁵ E. Shumilov,²⁹ A. Shvorob,³⁴ T. Siedenbarg,¹ D. Son,⁴⁴ A. Sopczak,⁴⁹ V. Soulimov,³⁰ B. Smith,¹⁶ P. Spillantini,¹⁷ M. Steuer,¹⁶ D. P. Stickland,³⁷ H. Stone,³⁷ B. Stoyanov,⁴³ A. Straessner,¹ K. Strauch,¹⁵ K. Sudhakar,¹⁰ G. Sultanov,¹⁹ L. Z. Sun,²¹ G. F. Susinno,²⁰ H. Suter,⁵⁰ J. D. Swain,¹⁹ X. W. Tang,⁷ L. Tauscher,⁶ L. Taylor,¹² Samuel C. C. Ting,¹⁶ S. M. Ting,¹⁶ M. Tonutti,¹ S. C. Tonwar,¹⁰ J. Tóth,¹⁴ C. Tully,³⁷ H. Tuchscherer,⁴⁵ K. L. Tung,⁷ Y. Uchida,¹⁶ J. Ulbricht,⁵⁰ U. Uwer,¹⁸ E. Valente,³⁸ R. T. Van de Walle,³² G. Vesztegombi,¹⁴ I. Vetlitsky,²⁹ G. Viertel,⁵⁰ M. Vivargent,⁴ R. Völkert,⁴⁹ H. Vogel,³⁶ H. Vogt,⁴⁹ I. Vorobiev,²⁹ A. A. Vorobyov,³⁹ A. Vorvolakos,³¹ M. Wadhwa,⁶ W. Wallraff,¹ J. C. Wang,¹⁶ X. L. Wang,²¹ Z. M. Wang,²¹ A. Weber,¹ F. Wittgenstein,¹⁸ S. X. Wu,¹⁹ S. Wynhoff,¹ J. Xu,¹¹ Z. Z. Xu,²¹ B. Z. Yang,²¹ C. G. Yang,⁷ X. Y. Yao,⁷ J. B. Ye,²¹ S. C. Yeh,⁵² J. M. You,³⁶ An. Zalite,³⁹ Yu. Zalite,³⁹ P. Zemp,⁵⁰ Y. Zeng,¹ Z. Zhang,⁷ Z. P. Zhang,²¹ B. Zhou,¹¹ Y. Zhou,³ G. Y. Zhu,⁷ R. Y. Zhu,³⁴ A. Zichichi,^{9,18,19} F. Ziegler.⁴⁹

- 1 I. Physikalisches Institut, RWTH, D-52056 Aachen, FRG[§]
III. Physikalisches Institut, RWTH, D-52056 Aachen, FRG[§]
 - 2 National Institute for High Energy Physics, NIKHEF, and University of Amsterdam, NL-1009 DB Amsterdam, The Netherlands
 - 3 University of Michigan, Ann Arbor, MI 48109, USA
 - 4 Laboratoire d'Annecy-le-Vieux de Physique des Particules, LAPP, IN2P3-CNRS, BP 110, F-74941 Annecy-le-Vieux CEDEX, France
 - 5 Johns Hopkins University, Baltimore, MD 21218, USA
 - 6 Institute of Physics, University of Basel, CH-4056 Basel, Switzerland
 - 7 Institute of High Energy Physics, IHEP, 100039 Beijing, China[△]
 - 8 Humboldt University, D-10099 Berlin, FRG[§]
 - 9 University of Bologna and INFN-Sezione di Bologna, I-40126 Bologna, Italy
 - 10 Tata Institute of Fundamental Research, Bombay 400 005, India
 - 11 Boston University, Boston, MA 02215, USA
 - 12 Northeastern University, Boston, MA 02115, USA
 - 13 Institute of Atomic Physics and University of Bucharest, R-76900 Bucharest, Romania
 - 14 Central Research Institute for Physics of the Hungarian Academy of Sciences, H-1525 Budapest 114, Hungary[‡]
 - 15 Harvard University, Cambridge, MA 02139, USA
 - 16 Massachusetts Institute of Technology, Cambridge, MA 02139, USA
 - 17 INFN Sezione di Firenze and University of Florence, I-50125 Florence, Italy
 - 18 European Laboratory for Particle Physics, CERN, CH-1211 Geneva 23, Switzerland
 - 19 World Laboratory, FBLJA Project, CH-1211 Geneva 23, Switzerland
 - 20 University of Geneva, CH-1211 Geneva 4, Switzerland
 - 21 Chinese University of Science and Technology, USTC, Hefei, Anhui 230 029, China[△]
 - 22 SEFT, Research Institute for High Energy Physics, P.O. Box 9, SF-00014 Helsinki, Finland
 - 23 University of Lausanne, CH-1015 Lausanne, Switzerland
 - 24 INFN-Sezione di Lecce and Università Degli Studi di Lecce, I-73100 Lecce, Italy
 - 25 Los Alamos National Laboratory, Los Alamos, NM 87544, USA
 - 26 Institut de Physique Nucléaire de Lyon, IN2P3-CNRS, Université Claude Bernard, F-69622 Villeurbanne, France
 - 27 Centro de Investigaciones Energeticas, Medioambientales y Tecnológicas, CIEMAT, E-28040 Madrid, Spain[‡]
 - 28 INFN-Sezione di Milano, I-20133 Milan, Italy
 - 29 Institute of Theoretical and Experimental Physics, ITEP, Moscow, Russia
 - 30 INFN-Sezione di Napoli and University of Naples, I-80125 Naples, Italy
 - 31 Department of Natural Sciences, University of Cyprus, Nicosia, Cyprus
 - 32 University of Nijmegen and NIKHEF, NL-6525 ED Nijmegen, The Netherlands
 - 33 Oak Ridge National Laboratory, Oak Ridge, TN 37831, USA
 - 34 California Institute of Technology, Pasadena, CA 91125, USA
 - 35 INFN-Sezione di Perugia and Università Degli Studi di Perugia, I-06100 Perugia, Italy
 - 36 Carnegie Mellon University, Pittsburgh, PA 15213, USA
 - 37 Princeton University, Princeton, NJ 08544, USA
 - 38 INFN-Sezione di Roma and University of Rome, "La Sapienza", I-00185 Rome, Italy
 - 39 Nuclear Physics Institute, St. Petersburg, Russia
 - 40 University and INFN, Salerno, I-84100 Salerno, Italy
 - 41 University of California, San Diego, CA 92093, USA
 - 42 Dept. de Física de Partículas Elementales, Univ. de Santiago, E-15706 Santiago de Compostela, Spain
 - 43 Bulgarian Academy of Sciences, Central Lab. of Mechatronics and Instrumentation, BU-1113 Sofia, Bulgaria
 - 44 Center for High Energy Physics, Korea Adv. Inst. of Sciences and Technology, 305-701 Taejeon, Republic of Korea
 - 45 University of Alabama, Tuscaloosa, AL 35486, USA
 - 46 Utrecht University and NIKHEF, NL-3584 CB Utrecht, The Netherlands
 - 47 Purdue University, West Lafayette, IN 47907, USA
 - 48 Paul Scherrer Institut, PSI, CH-5232 Villigen, Switzerland
 - 49 DESY-Institut für Hochenergiephysik, D-15738 Zeuthen, FRG
 - 50 Eidgenössische Technische Hochschule, ETH Zürich, CH-8093 Zürich, Switzerland
 - 51 University of Hamburg, D-22761 Hamburg, FRG
 - 52 High Energy Physics Group, Taiwan, China
- § Supported by the German Bundesministerium für Bildung, Wissenschaft, Forschung und Technologie
‡ Supported by the Hungarian OTKA fund under contract number T14459.
‡ Supported also by the Comisión Interministerial de Ciencia y Tecnología
‡ Also supported by CONICET and Universidad Nacional de La Plata, CC 67, 1900 La Plata, Argentina
◇ Also supported by Panjab University, Chandigarh-160014, India
△ Supported by the National Natural Science Foundation of China.

References

- [1] F. Boudjema *et al.*, “Z Physics at LEP 1”, V.2,ed. J.Ellis and R. Peccei, CERN 89-08 (1989) 188 and references therein.
- [2] L3 Collaboration, B. Adeva *et al.*, Phys. Lett. **B247** (1990) 177;
L3 Collaboration, B. Adeva *et al.*, Phys. Lett. **B250** (1990) 205;
L3 Collaboration, B. Adeva *et al.*, Phys. Lett. **B252** (1990) 525;
L3 Collaboration, O. Adriani *et al.*, Phys. Rep. **236** (1993) 1.
- [3] ALEPH Collaboration, D. Decamp *et al.*, Phys. Lett. **B236** (1990) 501;
ALEPH Collaboration, D. Decamp *et al.*, Phys. Lett. **B250** (1990) 172 ;
DELPHI Collaboration, P. Abreu *et al.*, Z. Phys. **C53** (1992) 41;
OPAL Collaboration, M.Z. Akrawy *et al.*, Phys. Lett. **B244** (1990) 135.
- [4] L3 Collaboration, M. Acciarri *et al.*, Phys. Lett. **B370** (1996) 211.
- [5] ALEPH Collaboration, D. Buskulic *et al.*, Phys. Lett. **B385** (1996) 445;
DELPHI Collaboration, P. Abreu *et al.*, Phys. Lett. **B380** (1996) 480;
OPAL Collaboration, G. Alexander *et al.*, Phys. Lett. **B386** (1996) 463.
- [6] H1 Collaboration, I. Abt *et al.*, Nucl. Phys. **B396** (1993) 3;
ZEUS Collaboration, M. Derrick *et al.*, Z. Phys. **C65** (1994) 627;
ZEUS Collaboration, M. Derrick *et al.*, Phys. Lett. **B316** (1993) 207.
- [7] K. Hagiwara *et al.*, Z.Phys. **C29** (1985) 115.
- [8] J. Bailey *et al.*, Phys. Lett. **B68** (1977) 191;
F. J. M. Farley, Z. Phys. **C56** (1992) S88;
F. M. Renard, Phys. Lett. **B116** (1982) 264;
F. de Aguila, A. Mendez and R. Pascual, Phys. Lett. **B140** (1984) 431;
M. Suzuki, Phys. Lett. **B143** (1984) 237.
- [9] H. Terazawa *et al.*, Phys. Lett. **B112** (1982) 387.
- [10] F. Boudjema and A. Djouadi, Phys. Lett. **B240** (1990) 485;
F. Boudjema, A. Djouadi and J.L Kneur, Z. Phys. **C57** (1993) 425;
M.B. Voloshin, *et al.*, Sov. Phys. JETP **64** (1986) 446;
M.B. Voloshin, Phys. Lett. **B209** (1988) 360.
- [11] S. Jadach, J. H. Kühn, Z. Was, Comp. Phys. Comm. **64** (1991) 275;
S. Jadach, B.F.L. Ward and Z. Was, Comp. Phys. Comm. **66** (1991) 276.
- [12] T. Sjöstrand, Comp. Phys. Comm. **39** (1986) 347;
T. Sjöstrand and M. Bengtsson, Comp. Phys. Comm. **43** (1987) 367.
- [13] The L3 detector simulation is based on GEANT Version 3.14, November 1990, see R. Brun *et al.*, “GEANT 3”, CERN DD/EE/84-1 (Revised), Sept. 1987.
The GHEISHA program (H. Fesefeldt, RWTH Aachen Report PITHA 85/02 (1985)) is used to simulate hadronic interactions.
- [14] L3 Collaboration, B. Adeva *et al.*, Nucl. Instr. and Meth. **A 289** (1990) 35.

- [15] O. Adriani et al., Nucl. Instr. and Meth. **A 302** (1991) 53.
- [16] M. Skrzypek, S. Jadach, W. Placzek and Z. Wąs, Comp. Phys. Comm. **94** (1996) 216-248.
- [17] D.Karlen, Nucl. Phys. **B289** (1987) 23.
- [18] F.A. Berends *et al.*, Nucl. Phys. **B301** (1988) 583.
- [19] F.A. Berends and R. Kleiss, Nucl. Phys. **B186** (1981) 22.
- [20] DELPHI Collaboration, P. Abreu et al., "Search for excited leptons in e^+e^- collisions at $\sqrt{s} = 161$ GeV", CERN-PPE/96-169, submitted to Phys. Lett. B;
OPAL Collaboration, K. Akerstaff et al., "Search for Excited Leptons in e^+e^- Collisions at $\sqrt{s} = 161$ GeV", CERN-PPE/96-138, submitted to Phys. Lett. B.

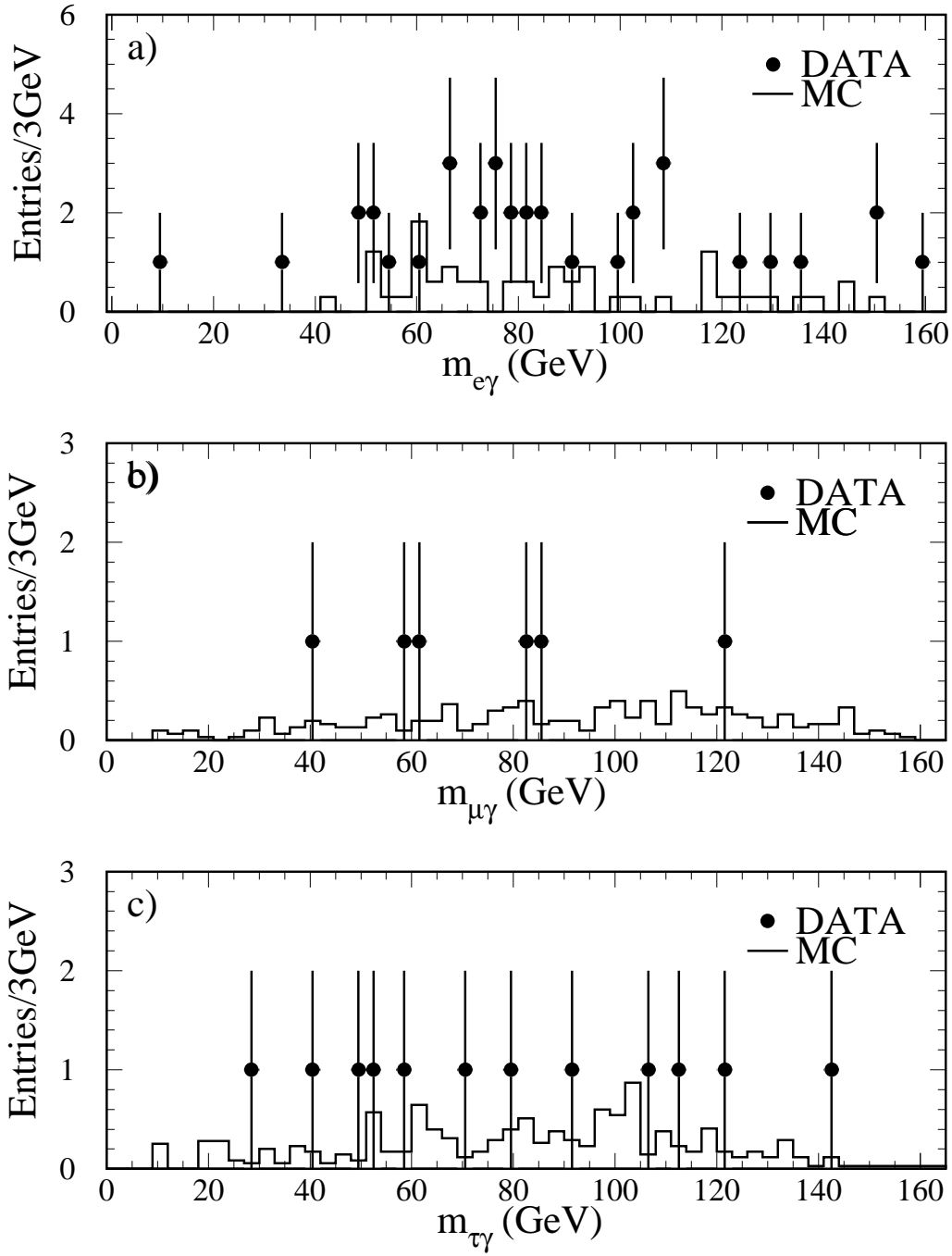


Figure 1: Selected events in single production searches: a) invariant mass of all $e\gamma$ combinations; b) invariant mass of all $\mu\gamma$ combinations; c) invariant mass of all $\tau\gamma$ combinations.

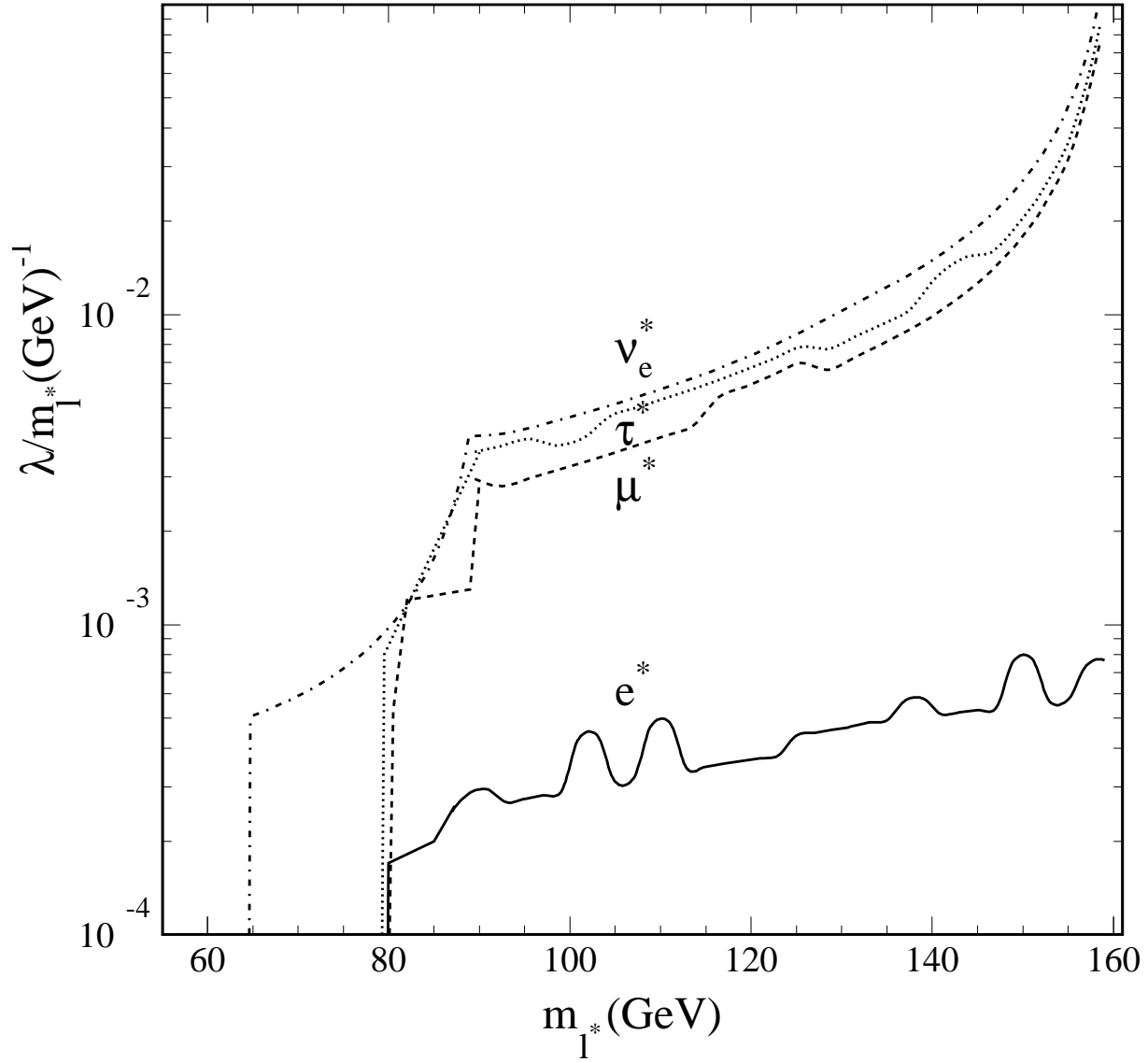


Figure 2: The upper limit of the coupling constant λ/m_{ℓ^*} at 95% C.L. as a function of m_{ℓ^*} for excited leptons with $f = f'$. The excluded region is above and to the left of the curves.

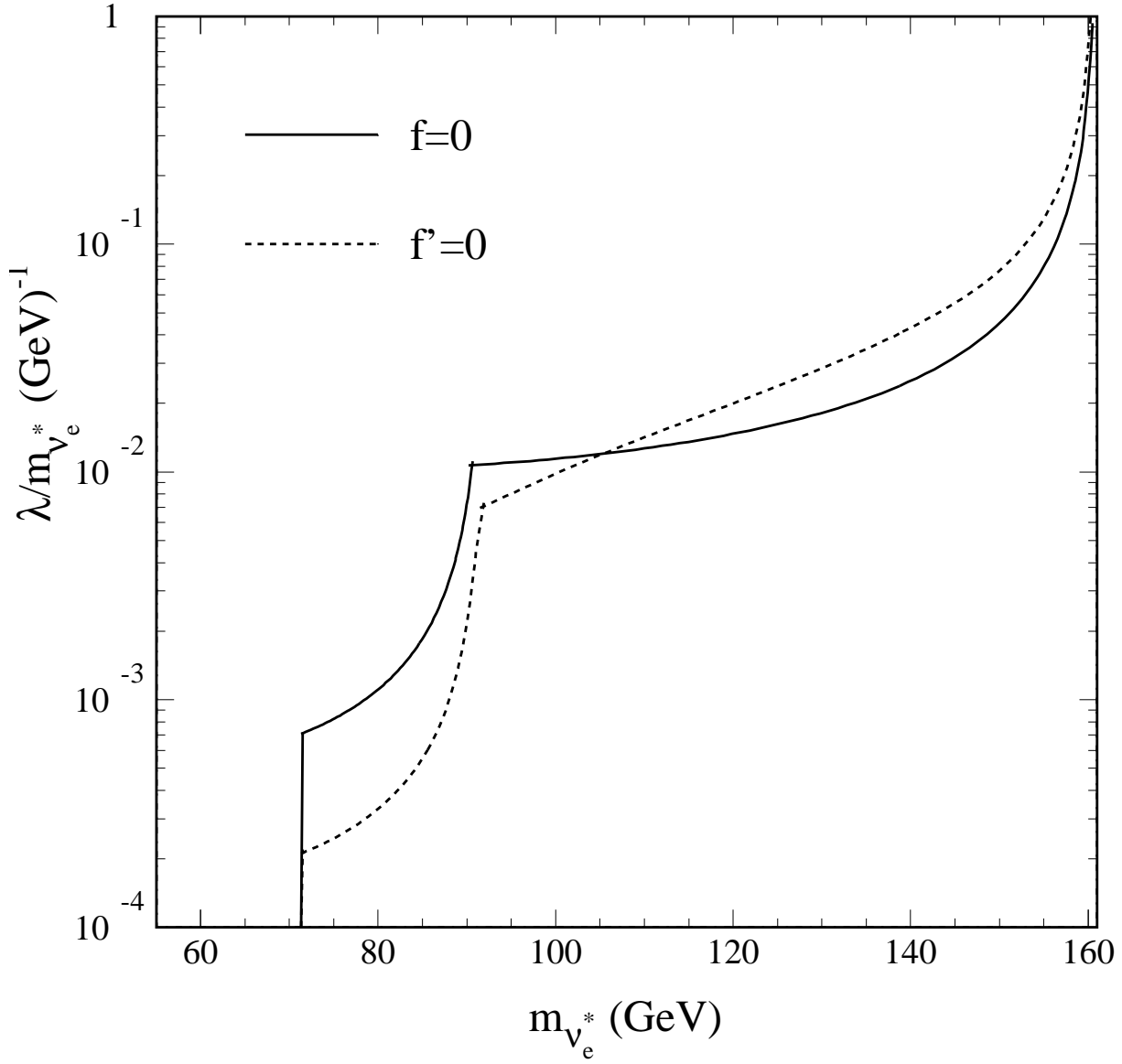


Figure 3: The upper limit of the coupling constant λ/m_{ℓ^*} at 95% C.L. as a function of m_{ℓ^*} for excited electron neutrinos with $\lambda = f$ ($f' = 0$) and $\lambda = f'$ ($f = 0$). The excluded region is above and to the left of the curves.